

Non-Convex Compressed Sensing Using Partial Support Information

Navid Ghadermarzy

Department of Mathematics, University of British Columbia
Vancouver, BC, Canada
navidgh@math.ubc.ca

Hassan Mansour *

Mitsubishi Electric Research Laboratories
Cambridge, MA 02139, USA
mansour@merl.com

Özgür Yılmaz

Department of Mathematics, University of British Columbia
Vancouver, BC, Canada
oyilmaz@math.ubc.ca

Abstract

In this paper we address the recovery conditions of weighted ℓ_p minimization for signal reconstruction from compressed sensing measurements when partial support information is available. We show that weighted ℓ_p minimization with $0 < p < 1$ is stable and robust under weaker sufficient conditions compared to weighted ℓ_1 minimization. Moreover, the sufficient recovery conditions of weighted ℓ_p are weaker than those of regular ℓ_p minimization if at least 50% of the support estimate is accurate. We also review some algorithms which exist to solve the non-convex ℓ_p problem and illustrate our results with numerical experiments.

Key words and phrases : Compressed sensing, Weighted ℓ_p , Nonconvex optimization, Sparse reconstruction

2000 AMS Mathematics Subject Classification — 94A12, 94A20, 94A08

*This work was conducted while Hassan Mansour was a postdoctoral research fellow in the Mathematics Department at the University of British Columbia.

1 Introduction

Compressed sensing is a data acquisition technique for efficiently recovering sparse signals from seemingly incomplete and noisy linear measurements. There are many applications where the target signals admit sparse or nearly sparse representations in some transform domain. For example, natural images are nearly sparse in discrete cosine transform domain (DCT) and in the wavelet domain. Similarly audio signals are approximately sparse in short time Fourier domain.

Compressed sensing is especially promising in applications where taking measurements is costly, e.g., hyperspectral imaging [9], as well as in applications where the ambient dimension of the signal is very large, i.e., medical [14] and seismic imaging [12].

Define $\Sigma_k^N := \{u \in \mathbb{R}^N : \|u\|_0 \leq k\}$ to be the set of all k -sparse vectors in \mathbb{R}^N — $\|u\|_0$ denotes the number of non-zero components of u . Let $x \in \Sigma_k^N$ and assume that $y \in \mathbb{R}^n$, the vector of n linear and potentially noisy measurements of x , is acquired via $y := Ax + e$ where e denotes the noise in our measurements with $\|e\|_2 \leq \epsilon$. Here A is an $n \times N$ measurement matrix with $n \ll N$. We wish to recover x from y by solving a sparse recovery problem. This entails finding the sparsest vector \hat{x} that is feasible, i.e., $\|A\hat{x} - y\| \leq \epsilon$. In the noise free case, i.e., $\epsilon = 0$, the decoder $\Delta_0 : \mathbb{R}^{n \times N} \times \mathbb{R}^n \mapsto \mathbb{R}^N$ is defined as

$$\Delta_0(A, y) := \underset{z \in \mathbb{R}^N}{\operatorname{argmin}} \|z\|_0 \quad \text{s.t.} \quad Az = y. \quad (1)$$

It was proved, e.g., in [8], that if $n > 2k$ and A is in general position, i.e., any collection of n columns of A is linearly independent, then $\Delta_0(A, y) = x$. However, (1) is a combinatorial problem which becomes intractable as the dimensions of the problem increase. Therefore, one seeks to modify the optimization problem so that it can be solved with methods that are more tractable than combinatorial search.

Donoho [7] and Candés, Romberg, and Tao [2] showed that if A obeys a certain “restricted isometry property”, solving a convex relaxation to the ℓ_0 problem can stably and robustly recover x from measurements $y = Ax + e$. More precisely, $\Delta_1 : \mathbb{R}^{n \times N} \times \mathbb{R}^n \times \mathbb{R} \mapsto \mathbb{R}^N$ is defined as

$$\Delta_1(A, y, \epsilon) := \underset{z \in \mathbb{R}^N}{\operatorname{argmin}} \|z\|_1 \quad \text{s.t.} \quad \|Az - y\| \leq \epsilon \quad (2)$$

The ℓ_1 minimization problem in (2) is a convex optimization problem and thus tractable. However, this computational tractability of ℓ_1 minimization comes at the cost of increasing the number of measurements taken. For example if columns of A are independent, identically distributed random vectors with any sub-Gaussian distribution, then Δ_1 can recover any k -sparse vector x when $n \gtrsim k \log(\frac{N}{k})$ rather than the $n > 2k$ property which is sufficient for recovery by Δ_0 .

Several works have attempted to close the gap in the required number of measurements for recovery via ℓ_0 and ℓ_1 minimization problems, including solving a non-convex ℓ_p minimization problem with $0 < p < 1$ [4, 10, 17] and using prior knowledge about the signal [11].

We will describe these in the next section. In this paper we propose to combine these approaches when there is prior information on the support of the signal. Specifically we introduce a weighted ℓ_p minimization algorithm and show that it outperforms both ℓ_p minimization and weighted ℓ_1 minimization under certain circumstances.

In Section 2, we briefly review various results on recovery by ℓ_1 , ℓ_p , and weighted ℓ_1 minimization. In Section 3, we describe the proposed recovery method based on weighted ℓ_p minimization, derive stability and robustness guarantees for this method and compare it with regular ℓ_p and weighted ℓ_1 . Specifically, we prove that the recovery guarantees for the weighted ℓ_p method with $0 < p < 1$ are better than those of weighted ℓ_1 and regular ℓ_p when we have a prior support estimate with accuracy better than 50%. In Section 4, we explain the algorithmic issues that come with solving the proposed non-convex optimization problem and the approach we take to empirically overcome them. Next, we present numerical experiments where we apply the weighted ℓ_p method to recover sparse and compressible signals. In Section 5, we show the result of applying these algorithms to audio signals and seismic data. In Section 6, we provide the proof for our main theorem.

2 Previous Work

In this section, we state the recovery algorithms based on ℓ_p and weighted ℓ_1 minimization, and the associated recovery guarantees. In both cases the restricted isometry constants play a central role.

Definition 1. A matrix A satisfies the restricted isometry property (RIP) of order k with constant δ_k if for all k -sparse vectors $z \in \Sigma_k^N$,

$$(1 - \delta_k) \|z\|_2^2 \leq \|Az\|_2^2 \leq (1 + \delta_k) \|z\|_2^2. \quad (3)$$

Recovery by ℓ_p Minimization

Chartrand [4], and Saab and Yılmaz [17], cf. [10], considered the sparse recovery method based on ℓ_p minimization with $0 < p < 1$. Here, the ℓ_1 norm in (2) is replaced by the ℓ_p quasi-norm. The decoder $\Delta_p : \mathbb{R}^{n \times N} \times \mathbb{R}^n \times \mathbb{R} \mapsto \mathbb{R}^N$ is defined as

$$\Delta_p(A, y, \epsilon) := \underset{z \in \mathbb{R}^N}{\operatorname{argmin}} \|z\|_p \quad \text{s.t.} \quad \|Az - y\| \leq \epsilon. \quad (4)$$

It was shown in [4, 10, 16, 17] that recovery by ℓ_p minimization is stable and robust under weaker sufficient conditions than the analogous conditions for recovery by ℓ_1 minimization. This result is made explicit by the following theorem from [17]. Note that setting $p = 1$ below yields the robust recovery theorem of Candés, Romberg and Tao [2] with identical sufficient conditions and constants.

Theorem 2. (Saab and Yilmaz [17]) Let k, N be positive integers with $k < N$ and $p \in (0, 1)$. Suppose that x is an arbitrary vector in \mathbb{R}^N and denote x_k by the best k -term approximation of x . Let $y = Ax + e$ with $\|e\|_2 \leq \epsilon$. If A satisfies $\delta_{ak} + a^{\frac{2}{p}-1} \delta_{(a+1)k} < a^{\frac{2}{p}-1} - 1$, for some $a \in \frac{1}{k}\mathbb{N}$, then

$$\|\Delta_p(A, y, \epsilon) - x\|_2^p \leq C_1^{\ell_p} \cdot \epsilon^p + C_2^{\ell_p} \cdot \frac{\|x - x_k\|_p^p}{k^{1-p/2}},$$

where $C_1^{\ell_p}$ and $C_2^{\ell_p}$ are given explicitly in [17, Th. 2.1].

Remark 3. It is sufficient that A satisfies

$$\delta_{(a+1)k} < \hat{\delta}^{\ell_p} := \frac{a^{\frac{2}{p}-1} - 1}{a^{\frac{2}{p}-1} + 1} \quad (5)$$

for Theorem 2 to hold (with same constants).

Remark 4. Proposition 2.10 in [17] has compared the recovery guarantees of Δ_1 and Δ_p in the noise free case. Assume there exists $k_1 > 1$ and $a \in \frac{1}{k_1}\mathbb{N}$ such that $\delta_{(a+1)k_1} < \frac{a-1}{a+1}$. Then a standard result [2, Theorem 1] guarantees that (2) can recover all k_1 -sparse signals and Theorem 2 guarantees that (4) can recover all k_p -sparse vectors where $k_p = \left\lfloor \frac{a+1}{a^{\frac{2}{p}-1} + 1} k_1 \right\rfloor$. Notice that $k_p > k_1$ when $p < 1$.

Recovery by Weighted ℓ_1 Minimization

The ℓ_1 problem (2) does not use any prior information about the signal. In many applications it is possible to obtain a partially accurate estimate of the support—the set of indices of the large coefficients—of the signal. It was noted in [11] that one can improve the recovery performance by incorporating the prior support information into the ℓ_1 -minimization-based recovery algorithm. In particular [11] proposes the weighted ℓ_1 decoder $\Delta_{1,w} : \mathbb{R}^{n \times N} \times \mathbb{R}^n \times \mathbb{R} \times \mathbb{R}^N \mapsto \mathbb{R}^N$ defined as

$$\Delta_{1,w}(A, y, \epsilon, w) := \operatorname{argmin}_{z \in \mathbb{R}^N} \|z\|_{1,w} \text{ s.t. } \|Az - y\| \leq \epsilon, \quad (6)$$

where $w \in \{\omega, 1\}^N$ is the weight vector and $\|z\|_{1,w} := \sum_i w_i |z_i|$ is the weighted ℓ_1 norm of z . Given a support estimate $\tilde{T} \subseteq \{1, \dots, N\}$ and assuming $w_j = \omega < 1$ for $j \in \tilde{T}$ and $w_j = 1$ for $j \notin \tilde{T}$, $\Delta_{1,w}$ enjoys better error bounds compared to Δ_1 provided \tilde{T} is sufficiently accurate. The following theorem was proved in [11].

Theorem 5. ([11]) Let x be an arbitrary vector in \mathbb{R}^N and $y = Ax + e$ with $\|e\|_2 \leq \epsilon$. Denote x_k by the best k -term approximation of x with $\operatorname{supp}\{x_k\} = T_0$. Let \tilde{T} be an arbitrary subset of $\{1, 2, \dots, N\}$ and define ρ and α such that $|\tilde{T}| = \rho k$ and $|T_0 \cap \tilde{T}| =$

$\alpha\rho k$. Suppose there exists an $a \in \frac{1}{k}\mathbb{Z}$ with $a \geq (1-\alpha)\rho$ and $a > 1$ and the measurement matrix A has RIP with

$$\delta_{ak} + \frac{a}{(\omega + (1-\omega)\sqrt{1+\rho-2\alpha\rho})^2} \delta_{(a+1)k} < \frac{a}{(\omega + (1-\omega)\sqrt{1+\rho-2\alpha\rho})^2} - 1$$

for some $0 \leq \omega \leq 1$. Then

$$\|\Delta_{1,\omega}(A, y, \epsilon, \mathbf{w}) - x\|_2 \leq C_1^{\omega\ell_1} \epsilon + C_2^{\omega\ell_1} k^{\frac{-1}{2}} (\omega \|x - x_k\|_1 + (1-\omega) \|x_{\tilde{T}^c \cap T_0^c}\|_1),$$

where $C_1^{\omega\ell_1}$ and $C_2^{\omega\ell_1}$ are given explicitly in [11, Remark 3.1].

Remark 6. It is sufficient that A satisfies

$$\delta_{(a+1)k} < \hat{\delta}^{\omega\ell_1} := \frac{a - (\omega + (1-\omega)\sqrt{1+\rho-2\alpha\rho})^2}{a + (\omega + (1-\omega)\sqrt{1+\rho-2\alpha\rho})^2} \quad (7)$$

for Theorem 5 to hold (with same constants).

3 Main Results

In this section we introduce the decoder $\Delta_{p,\omega}$ that is based on weighted ℓ_p minimization. For a given prior support estimate \tilde{T} , $\Delta_{p,\omega} : \mathbb{R}^{n \times N} \times \mathbb{R}^n \times \mathbb{R} \times \mathbb{R}^N \mapsto \mathbb{R}^N$ is defined as

$$\Delta_{p,\omega}(A, y, \epsilon, \mathbf{w}) := \underset{z \in \mathbb{R}^N}{\operatorname{argmin}} \|z\|_{p,\mathbf{w}} \text{ s.t. } \|Az - y\| \leq \epsilon \text{ with } \mathbf{w}_i = \begin{cases} 1, & \text{if } i \in \tilde{T}^c \\ \omega, & \text{if } i \in \tilde{T} \end{cases}. \quad (8)$$

Here $\mathbf{w} \in \{\omega, 1\}^N$ is the weight vector and $\|z\|_{p,\mathbf{w}} := (\sum_i \mathbf{w}_i^p |z_i|^p)^{\frac{1}{p}}$ is the weighted ℓ_p norm. Next we provide the stable and robust recovery conditions of this algorithm and compare it with weighted ℓ_1 and ℓ_p .

3.1 Weighted ℓ_p Minimization with Estimated Support

As mentioned in the previous section, one can improve the recovery guarantees of Δ_1 by using Δ_p and by incorporating prior support information into the optimization problem. In this section we provide the recovery conditions when we combine both these approaches. The following theorem states the main result.

Theorem 7. *Let x be an arbitrary vector in \mathbb{R}^N and $y = Ax + e$ with $\|e\|_2 \leq \epsilon$. Denote x_k by the best k -term approximation of x with $\operatorname{supp}\{x_k\} = T_0$. Let \tilde{T} be an arbitrary subset of $\{1, 2, \dots, N\}$ and define ρ and α such that $|\tilde{T}| = \rho k$ and $|T_0 \cap \tilde{T}| = \alpha\rho k$.*

Suppose there exist an $a \in \frac{1}{k}\mathbb{Z}$, with $a \geq (1 - \alpha)\rho$ and $a > 1$ and the measurement matrix A has RIP with

$$\delta_{ak} + \frac{a^{\frac{2}{p}-1}}{(\omega^p + (1 - \omega^p)(1 + \rho - 2\alpha\rho)^{1-\frac{p}{2}})^{\frac{2}{p}}} \delta_{(a+1)k} < \frac{a^{\frac{2}{p}-1}}{(\omega^p + (1 - \omega^p)(1 + \rho - 2\alpha\rho)^{1-\frac{p}{2}})^{\frac{2}{p}}} - 1,$$

for some $0 \leq \omega \leq 1$ and $0 < p < 1$. Then

$$\|\Delta_{p,w}(A, y, \epsilon, \mathbf{w}) - x\|_2^p \leq C_1 \epsilon^p + C_2 k^{\frac{p}{2}-1} (\omega^p \|x - x_k\|_p^p + (1 - \omega^p) \|x_{\tilde{T}^c \cap T_0^c}\|_p^p). \quad (9)$$

Remark 8. Note that ρ denotes the ratio of the size of the estimated support to the size of the actual support of x_k and α denotes the accuracy of our estimate which is the ratio of the size of $\tilde{T} \cap T_0$, to the size of our estimate \tilde{T} .

Remark 9. The constants C_1 and C_2 are explicitly given in (24) in Section 6.

Remark 10. It is sufficient that A satisfies

$$\delta_{(a+1)k} < \hat{\delta}^{w\ell_p} := \frac{a^{\frac{2}{p}-1} - (\omega^p + (1 - \omega^p)(1 + \rho - 2\alpha\rho)^{1-\frac{p}{2}})^{\frac{2}{p}}}{a^{\frac{2}{p}-1} + (\omega^p + (1 - \omega^p)(1 + \rho - 2\alpha\rho)^{1-\frac{p}{2}})^{\frac{2}{p}}} \quad (10)$$

for Theorem 7 to hold, i.e., to guarantee stable and robust recovery described in the theorem with same constants C_1 and C_2 . Setting $\omega = 1$ gives us the sufficient conditions for recovery by Δ_p and setting $p = 1$ derives the sufficient recovery conditions for recovery by $\Delta_{1,w}$. Notice that these conditions are in terms of bounds on RIP constants. In the remainder of this section we compare these bounds.

3.2 Comparison with Weighted ℓ_1 Recovery

In this section we compare the conditions for which Theorem 7 holds with the corresponding conditions of Theorem 5. Following observation is easy to verify.

Proposition 11. Let $C_1, C_2, C_1^{w\ell_1}$ and $C_2^{w\ell_1}$ be as defined above. If $p = 1$ then $C_1 = C_1^{w\ell_1}$ and $C_2 = C_2^{w\ell_1}$ and the sufficient condition for Theorem 7 would be identical to Theorem 5.

Figure 1 illustrates how the sufficient conditions on the RIP constants vary with α and ω in the case of weighted ℓ_1 and weighted ℓ_p . In particular these sufficient conditions are introduced in Theorem 5 and Theorem 7, i.e., $\hat{\delta}^{w\ell_1}$ defined in (7) and $\hat{\delta}^{w\ell_p}$ defined in (10) which determine bounds on the RIP constants. Here we plot $\hat{\delta}^{w\ell_p}$ versus ω for weighted ℓ_1 ($p = 1$) and weighted ℓ_p ($0 < p < 1$) with different values of α when $a = 3$ and $p = \frac{2}{5}$. The bounds on RIP constants gets larger as α increases. Note that when $\alpha = 0.5$ the sufficient conditions for recovery by weighted ℓ_p would be identical to sufficient conditions for recovery by standard ℓ_p for $0 < p < 1$. Comparing these results with recovery by weighted ℓ_1 , we see that in recovery by weighted ℓ_p the measurement matrix A has to

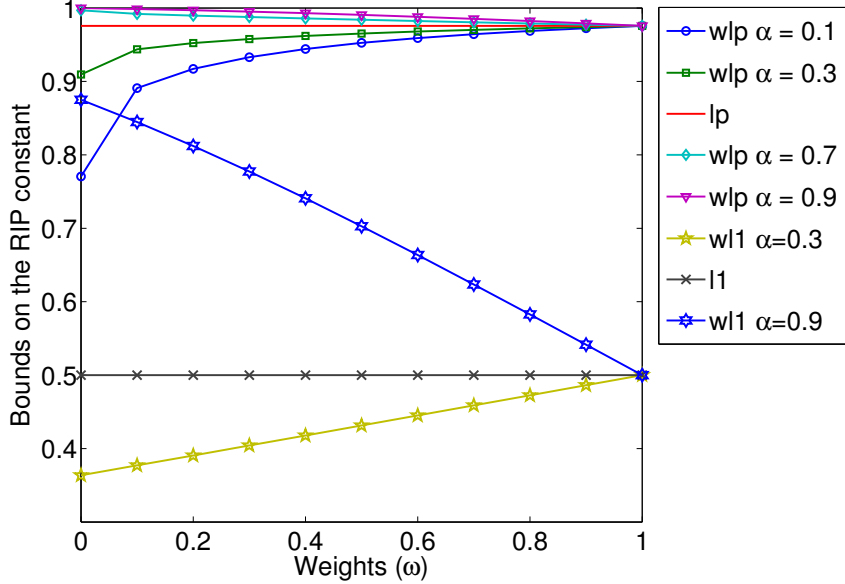

 (a) $\hat{\delta}^{w\ell_p}$ vs ω

Figure 1: Comparison of the sufficient conditions for recovery with weighted ℓ_p reconstruction with various α . In all figures, we set $a = 3$ and $\rho = 1$ and $p = \frac{2}{5}$.

satisfy much weaker conditions than the analogous conditions in recovery by weighted ℓ_1 even when we do not have a good support estimate. It is worth comparing the sufficient recovery conditions for the special case of zero weight. As seen in Figure 1 setting $\omega = 0$ is beneficial when $\alpha > 0.5$. Figure 2 compares the recovery guarantees we obtain in the zero-weight case for weighted ℓ_p and weighted ℓ_1 minimization. Specifically, we present the phase diagrams of measurement matrices A with Gaussian entries that satisfy the conditions on the restricted isometry constants $\delta_{(a+1)k}$ given in (7) and (10) with $\omega = 0$, $\rho = 1$, and $\alpha = 0.3, 0.6$, and 0.8 . Phase diagrams are calculated using the upper bounds on the RIP constants derived in [1] and reflect the sparsity levels for which the theorems guarantee exact signal recovery as a function of the aspect ratio of the measurement matrix A .

3.3 Comparison with ℓ_p Recovery

In this section we compare the sufficient conditions of Theorem 2 and Theorem 7. The following is easy to check.

Proposition 12. Let $C_1, C_2, C_1^{\ell_p}$ and $C_2^{\ell_p}$ be as defined above .

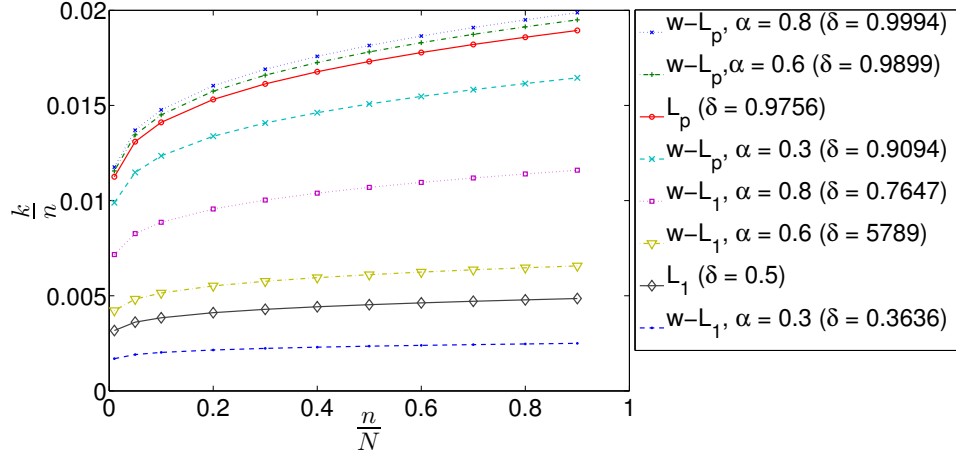


Figure 2: Comparison between phase diagrams of measurement matrices with Gaussian entries satisfying the sufficient recovery conditions of weighted ℓ_p and weighted ℓ_1 minimization with $\omega = 0$. Points below each curve determine the sparsity-undersampling ratios that satisfy the sufficient bounds on the RIP constants introduced in (7) and (10).

- (i) If $\alpha = 0.5$ then again $C_1 = C_1^{\ell_p}$ and $C_2 = C_2^{\ell_p}$ and the sufficient condition for Theorem 7 would be identical to Theorem 2.
- (ii) Suppose $0 \leq \omega < 1$. Then $C_1 < C_1^{\ell_p}$ and $C_2 < C_2^{\ell_p}$ if and only if $\alpha > 0.5$

Proposition 12 reflects the results shown in Figure 3. Figures 3.a and 3.b show how constants C_1 and C_2 in (9) change with ω for different values of α . Notice that constants decrease when we increase α .

When $\alpha < 0.5$, i.e., when our estimate is less than 50% accurate, using bigger weights results in more robust recovery, which is useful when the accuracy of the estimate is not guaranteed to be high. For all values of $\omega < 1$, having a support estimate accuracy $\alpha > 0.5$ results in a weaker condition on the RIP constant and smaller error bound constants compared with the conditions of standard ℓ_p . On the other hand, if $\alpha < 0.5$, i.e., the support estimate has low accuracy, then standard ℓ_p has weaker sufficient recovery conditions and smaller error bound constants compared to weighted ℓ_p . This behaviour is similar to that derived for weighted ℓ_1 minimization in [11].

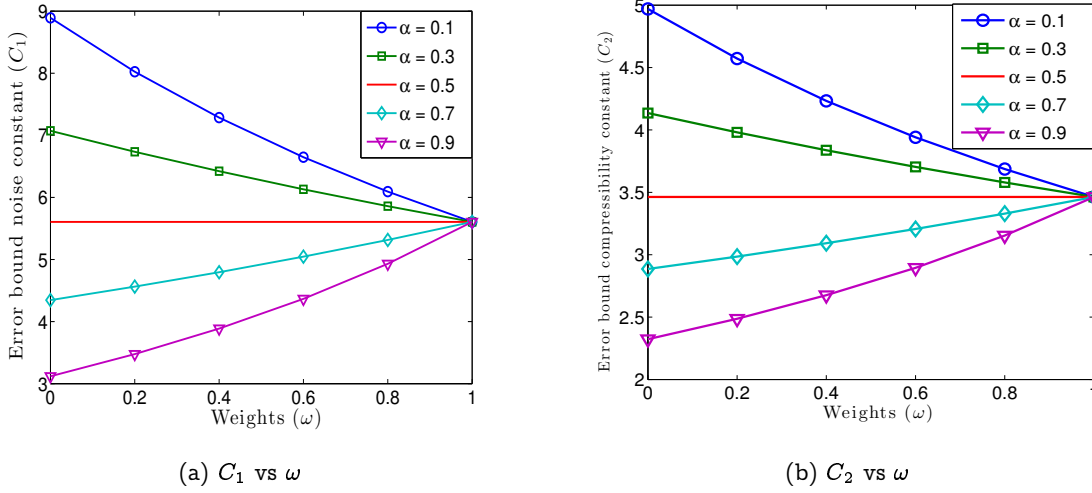


Figure 3: Comparison of the recovery constants for weighted ℓ_p reconstruction with various α . In all the Figures, we set $a = 3$ and $\rho = 1$ and $p = \frac{2}{5}$.

4 Numerical Experiments

4.1 Algorithmic Issues

Before we present numerical experiments, we describe the algorithm that we used to approximate $\Delta_{p,w}$, i.e., to “solve” the weighted ℓ_p minimization problem.

To this day, there is no algorithm that provably solves this non-convex optimization problem. On the other hand, there are a few algorithms which are commonly used to attempt to solve this minimization problem. These include simple modifications of well-known algorithms such as the projected gradient method [4], the iterative reweighted ℓ_1 method [5], and the iterative reweighted least squares method [3]. Since the ℓ_p minimization problem is non-convex and several local minima exist, these algorithms attempt to converge to local minima that are close to the global minimizer of the problem. To that end, the only proofs of global convergence that currently exist assume that the global minimizer can be found if a feasible point can be found. However, numerical experiments show that these algorithms perform well, for example, when the measurement matrix has i.i.d. Gaussian random entries. To produce the numerical experiments below, we have used the projected gradient method which is described next.

The algorithm starts by minimizing a smoothed ℓ_p objective given by $(\sum_i (x_i^2 + \sigma)^{p/2})^{1/p}$ instead of of the ℓ_p norm. The smoothing parameter σ is initialized with a large value of 10. The algorithm follows by taking a projected gradient step and reducing the value of σ . In every iteration, the new iterant is projected onto the affine space $Ax = b$. Algorithm 1

explains the details of this algorithm. Here $\nabla(f_x)_i = p \times w_i^p \times (x_i^{(t)} \times (x_i^{(t)})^* + \sigma^2)^{p/2-1} \times x_i^{(t)}$.

Algorithm 1 Modified projected gradient method

- 1: **Input** $b = Ax + e$, p , A , $w_i \in [0, 1]$ for all $i \in 1 \dots N$
 - 2: **Output** $x^{(t)}$
 - 3: **Initialize** $\sigma = 10$, $t = 0$, $x^{(0)} = A^H b$, $[M \ N] = \text{size}(A)$, $Q = A^\dagger \times A$, $w_i = \begin{cases} w, & i \in \Lambda \\ 1, & i \in \Lambda^c \end{cases}$
 - 4: **loop**
 - 5: $f_x = \sum_i (w_i^2 \times (x_i^{(t)^2} + \sigma))^{p/2}$
 - 6: $d = -\nabla(f_x)$
 - 7: $pd = d - Q \times d$
 - 8: $t = t + 1$
 - 9: line search
 - 10: $x^{(t)} = x^{(t-1)} + l \times pd$
 - 11: $\text{Indicator} = \frac{\sqrt{1-p} \times x^{(t)}}{1-\sqrt{p}}$
 - 12: $\text{Idx} = \text{find}(\text{Indicator} < w \times \sigma)$
 - 13: $\sigma = \min(0.98 \times \sigma, \max(\text{Indicator}))$
 - 14: **end loop**
-

Next, we provide numerical results to show how $\Delta_{p,w}$ improves the recovery conditions of sparse and approximately sparse signals compared to Δ_p and $\Delta_{1,w}$. We show the results for sparse and compressible signals where we use Algorithms 1 to solve the weighted ℓ_p minimization problem.

4.2 Numerical Experiments: The Sparse Case

In this section, we compare the performance of $\Delta_{1,w}$ in recovering exactly sparse signals for various values of p and weight w including $p = 1$, which corresponds to weighted ℓ_1 of [11] and $w = [1, 1, \dots, 1]^T$, which corresponds to ℓ_p minimization. Specifically, we create 40-sparse signals $x \in \mathbb{R}^{500}$, and obtain (noisy) compressed measurements of x via $y = Ax + e$ where A is chosen to be an $n \times 500$ Gaussian matrix with n varying between 80 and 200. In the case of noisy measurements, e is drawn from uniform distribution on the sphere and normalized such that $\frac{\|e\|_2}{\|x\|_2} = 0.05$. Figure 4 shows the reconstruction signal-to-noise ratio (SNR) averaged over 10 experiments as a function of the number of the measurements obtained using weighted ℓ_p and weighted ℓ_1 minimization. Figures 4.a and 4.b show the noise-free case and the noisy case, respectively. In both scenarios, we try different levels of prior support estimate accuracy α , i.e., $\alpha \in \{0.3, 0.5, 0.7\}$ with weighted

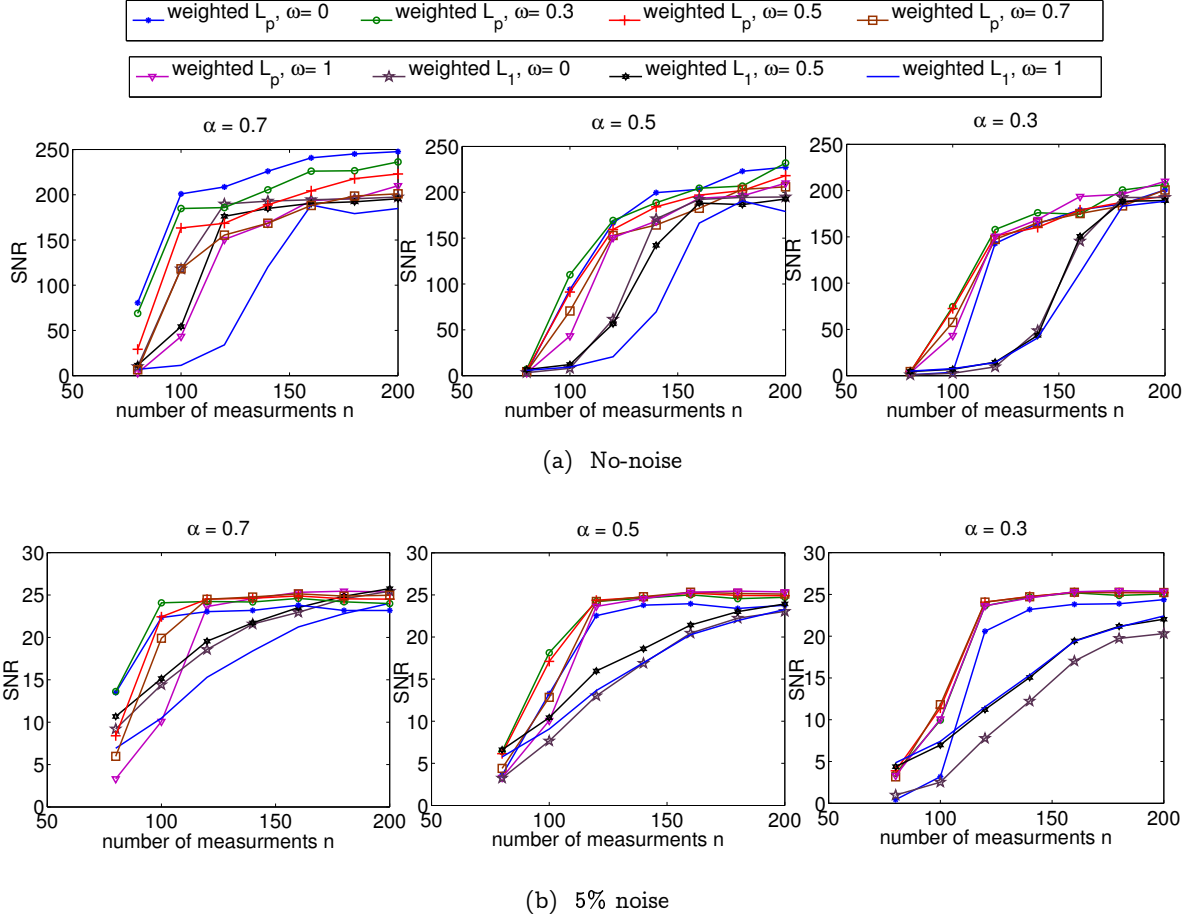


Figure 4: Comparison of Performance of weighted ℓ_p and weighted ℓ_1 recovery in terms of SNR averaged over 10 experiments for sparse signals with variable weights and measurements and $\rho = 1$ and $p = 0.5$.

ℓ_p ($p = 0.5$) and weighted ℓ_1 . Here the SNR is measured in dB and is given by

$$\text{SNR}(x, \hat{x}) = 10 \log_{10} \left(\frac{\|x\|_2^2}{\|x - \hat{x}\|_2^2} \right). \quad (11)$$

Figure 4.a illustrates that, in the noise free case, the experimental results are consistent with the theoretical results derived in Theorem 7. More precisely, when $\alpha > 0.5$ the best recovery is achieved when the weights are set to zero and as α decreases, the best recovery is achieved when larger weights are used. Also weighted ℓ_p is recovering significantly better than weighted ℓ_1 , especially when we have few measurements, which is consistent with our

analysis in Section 3.

Remark 13. In Figures 1 and 3 we can see that when $\alpha < 0.5$ both the sufficient recovery conditions and error bound constants point towards using $\omega = 1$. However, Figure 4 suggests that this is not always true. We attribute this behavior to the best k -term approximation term in the error bound of Theorem 7. Consider the noise free case where the error bound becomes $\|x^* - x\|_2^p \leq C_2 k^{\frac{p}{2}-1} (\omega^p \|x - x_k\|_p^p + (1 - \omega^p) \|x_{\tilde{T}^c \cap T_0^c}\|_p^p)$. Notice that on T_0^c , $x_k = 0$ so we have $\|x_{\tilde{T}^c \cap T_0^c}\| = \|(x - x_k)_{\tilde{T}^c \cap T_0^c}\|$ which means that $\|x_{\tilde{T}^c \cap T_0^c}\|_p^p \leq \|x - x_k\|_p^p$. Therefore, increasing ω increases $\omega^p \|x - x_k\|_p^p + (1 - \omega^p) \|x_{\tilde{T}^c \cap T_0^c}\|_p^p$. On the other hand, as we can see in Figure 3, the constant C_2 decreases as ω increases. Consequently when the algorithm cannot recover the full support of x , i.e., when $\|x - x_k\| > 0$, an intermediate value of ω in $(0, 1)$ may result in the smallest recovery error. A full mathematical analysis of the above observations needs to take into account all the interdependencies between ω, k, α and the parameters in Theorem 7 which is beyond the scope of this paper. Figure 4.b shows results for the noisy case. Using intermediate weights results in best recovery and weighted ℓ_p is outperforming weighted ℓ_1 especially when we have few measurements.

4.3 Numerical Experiments: The Compressible Case

In this section we consider signals $x \in \mathbb{R}^{500}$ such that $x_j = j^{-d}$ for some $d > 1$. Figure 5 shows the average SNR over 20 experiments—20 Gaussian measurement matrices A with the same signal x —when $n = 100$ and $d = 1.1$. We generate support estimates that target to find the locations of the largest 40 entries of x , i.e., a support estimate with accuracy $\alpha = 1$ and relative size $\rho = 1$ is $\{1, \dots, 40\}$. Figure 5.a shows the no-noise case and Figure 5.b has 5% noise. As we can see using intermediate weights results in better reconstruction. When the measurements are noisy, unlike the sparse case, using weighted ℓ_p for recovering compressible signals doesn't give us much better results than weighted ℓ_1 , specifically in Figure 5.b when $\alpha = 0.7$ we see that weighted ℓ_1 with zero weight is recovering better than weighted ℓ_p . We believe that this is a result of the algorithm we are using. As we said before we don't have any proof for global convergence of the algorithm and the projected gradient algorithm handles the local minima by a smoothing parameter σ . In the noisy compressible case we have lots of these local minimums which may be a reason that in some of the compressible noisy cases we see that weighted ℓ_1 is recovering better than weighted ℓ_p .

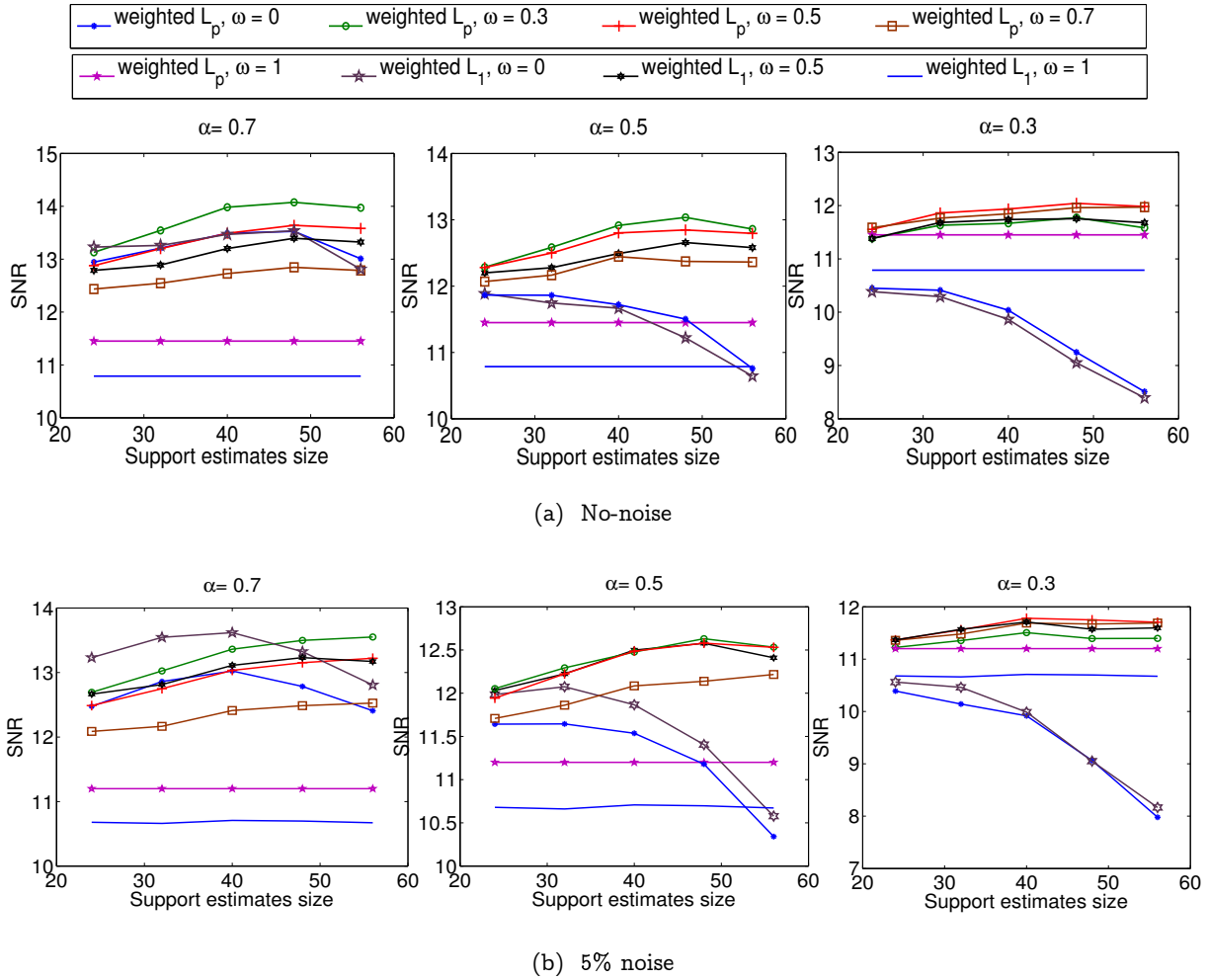


Figure 5: Comparison of performance of weighted ℓ_p and weighted ℓ_1 recovery in terms of SNR averaged over 20 experiments for compressible signals x with $n = 100, N = 500$. The coefficients decay with a power $d = 1.1$. The accuracy of the support estimate α is calculated with respect to the best $k = 40$ term approximation.

5 Stylized Applications

In this section, we apply standard and weighted ℓ_p minimization to recover real audio and seismic signals that are compressively sampled.

5.1 Audio Signals

In this section we examine the performance of weighted ℓ_p minimization for the recovery of compressed sensing measurements of speech signals. Here the speech signals are sampled at 44.1 kHz and we randomly choose only $\frac{1}{4}$ th of the samples. Assuming that s is the speech signal, we obtain the measurements $y = Rs$ where R is a restriction of the identity operator.

We divide our measurements y into 21 blocks, i.e., $y = [y_1^T, y_2^T, \dots]^T$. Assuming the speech signal is compressible in DCT domain, we try to recover it using each block measurement. Doing this reduces the size of the problem and considering the fact that the support set corresponding to the largest coefficients doesn't change much from one block to another, we can use the indices of the largest coefficients of each block as a support estimate for the next one. For each block, we find the speech signal by solving $y_j = R_j s_j$, where $R_j \in \mathbb{R}^{n_j \times N}$ is the associated restriction matrix. We also know that speech signals have large low-frequency coefficients, so we use this fact and the recovered signal at previous block to build our support estimate and find the speech signal at each block by weighted ℓ_p minimization. We choose the support estimate to be $\tilde{T} = \tilde{T}^1 \cup \tilde{T}^2$, where \tilde{T}^1 is the set corresponding to frequencies up to 4 kHz and \tilde{T}^2 is the set corresponding to the largest $\frac{n_j}{16}$ recovered coefficients of the previous block—for the first block \tilde{T}^2 is empty. The results of using weighted ℓ_p and weighted ℓ_1 for reconstruction two audio signals—one male and one female—are illustrated in Figure 6. Here $N = 2048$, and $\omega \in 0, \frac{1}{6}, \frac{2}{6}, \dots, 1$. Weighted ℓ_p gives about 1-dB improvement in reconstruction.

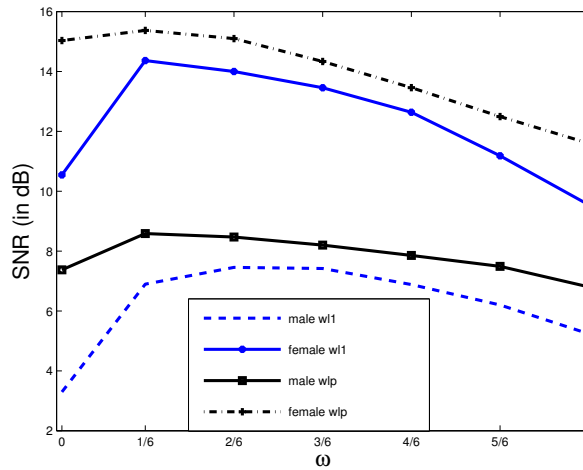


Figure 6: SNRs of reconstructed audio signals from compressed sensing measurements plotted against ω via weighted ℓ_1 weighted ℓ_p with $p = \frac{1}{2}$. An intermediate value of ω yields the best performance.

5.2 Seismic Signals

The problem of interpolating irregularly sampled and incomplete seismic data to a regular periodic grid often occurs in 2D and 3D seismic settings [15]. Assume that we have N_s sources located on earth surface which send sound waves into the earth and N_r receivers record the reflection in N_t time samples. Hence the seismic data is organized in a 3-D seismic line with N_s sources, N_r receivers, and N_t time samples. Rearranging the seismic line, we have a signal $f \in \mathbb{R}^N$, where $N = N_s N_r N_t$. Assume $x = Sf$ where x is the sparse representation of f in curvelet domain. We want to recover a very high dimensional seismic data volume $f = S^*x$ by interpolating between a smaller number of measurements $b = RMS^*x$, where R is a restriction matrix, M represents the basis in which the measurements are taken, and S is the 2D curvelet transform. Seismic data is approximately sparse in curvelet domain and hence the interpolation problem becomes that of finding the curvelet synthesis coefficients with the smallest ℓ_1 norm that best fits the randomly subsampled data in the physical domain [6, 13]. We partition the seismic data volume into frequency slices and approximate $x^{(1)}$ by $\tilde{x}^{(1)} := \Delta_p(R^{(1)}MS^*, b^{(1)}, \epsilon)$ where ϵ is a small number (estimate of the noise level) and $R^{(1)}$ is the subsampling operator restricted to the first partition and $b^{(1)}$ is the subsampled measurements of the data $f^{(1)}$ in the first partition. After this we use the support of each recovered partition as a support estimate for next partition. In particular for $j \geq 1$ we approximate $x^{(j+1)}$ by $\tilde{x}^{(j+1)} := \Delta_{p,w}(R^{(j)}MS^H, b^{(j)}, \epsilon, w)$ where w is the weight vector which puts smaller weights on the coefficients that correspond to the support of the previous recovered partition. In [15] the performance of weighted ℓ_1 minimization has been tested for recovering a seismic line using 50% randomly subsampled receivers. Exploiting the ideas in [15] we test the weighted ℓ_p minimization algorithm to recover a test seismic problem when we subsample 50% of the the receivers using the mask shown in Figure 7.b. We omit the details of this algorithm as it mimics the steps taken in [15] when weighted ℓ_1 is replaced by weighted ℓ_p .

The seismic line at full resolution has $N_s = 64$ sources, $N_r = 64$ receivers with a sample distance of 12.5 meters, and $N_t = 256$ time samples acquired with a sampling interval of 4 milliseconds. Consequently, it contains samples collected in a 1s temporal window with a maximum frequency of 125 Hz. To access frequency slices, we take the one dimensional discrete Fourier transform (DFT) of the data along the time axis. We solve the ℓ_p and weighted ℓ_p minimization problems. In the $j + 1$ -th partition, the support estimate set is derived from the largest analysis coefficients $SS^H\tilde{x}^{(j)}$ of the previously recovered partition. Moreover, p is set to be 0.5 and the weight is set to 0.3.

Figures 8.a and 8.b show a fully sampled and the corresponding subsampled shot gather, respectively. The shot gather corresponds to shot number 32 of the seismic line. Figures 9.a and 9.b show the reconstructed shot gathers using ℓ_1 minimization and ℓ_p minimization, respectively and Figures 11.a and 11.b show the reconstructed shot gathers using weighted ℓ_1 minimization and weighted ℓ_p minimization, respectively. Furthermore the reconstruction error plots of ℓ_1 and ℓ_p minimization is showed in Figure 10.a and 10.b and

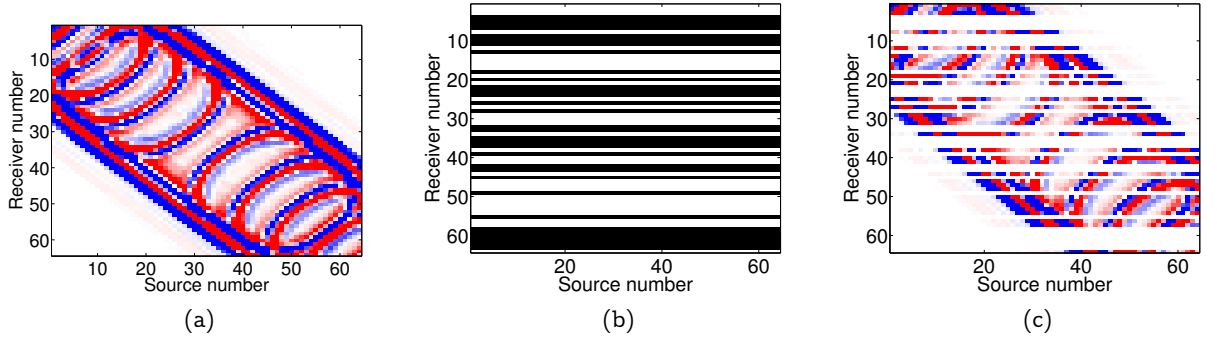


Figure 7: (a) Example of a high resolution time slice at $t = 0.32s$ in the source-receiver domain, (b) the random subsampling mask where the black lines correspond to the locations of inactive receivers, and (c) the subsampled time slice. Subsampling ratio is 50%.

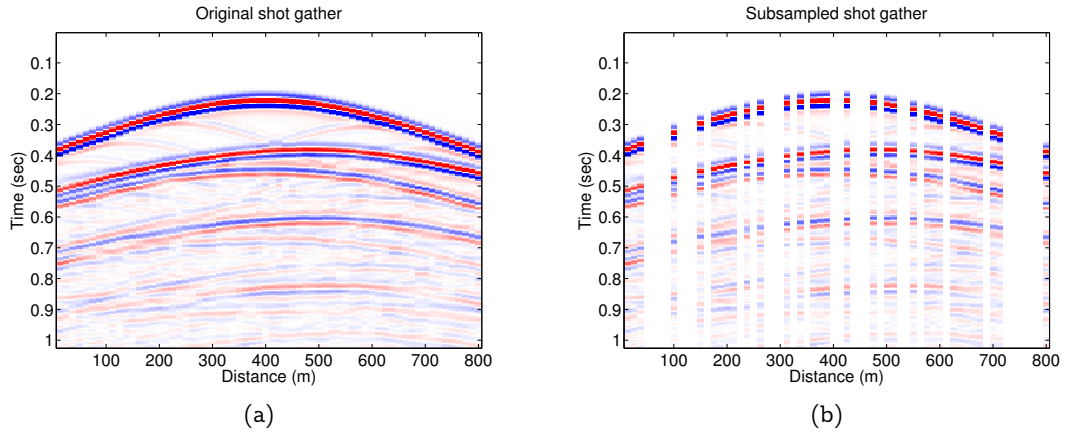


Figure 8: (a) Shot gather number 32 from the seismic line. (b) Subsampled shot gather using column 32 from the mask in Figure 7.b.

the reconstruction error plots of weighted ℓ_1 and weighted ℓ_p minimization are shown in Figures 12.a and 12.b.

Figure 13 shows the SNRs of all shot gathers recovered by using regular and weighted and regular ℓ_p and ℓ_1 minimization problems. The plots demonstrate that recovery by weighted ℓ_p in the frequency-source-receiver domain is always better than recovery by regular ℓ_p . In this plot we also see that although recovery by weighted ℓ_p minimization is better than regular ℓ_1 minimization but the results are just a little better than recovery by weighted ℓ_1 minimization. We believe that similar to the case we see in the noisy compressible case this is an artifact of the algorithm we are using.

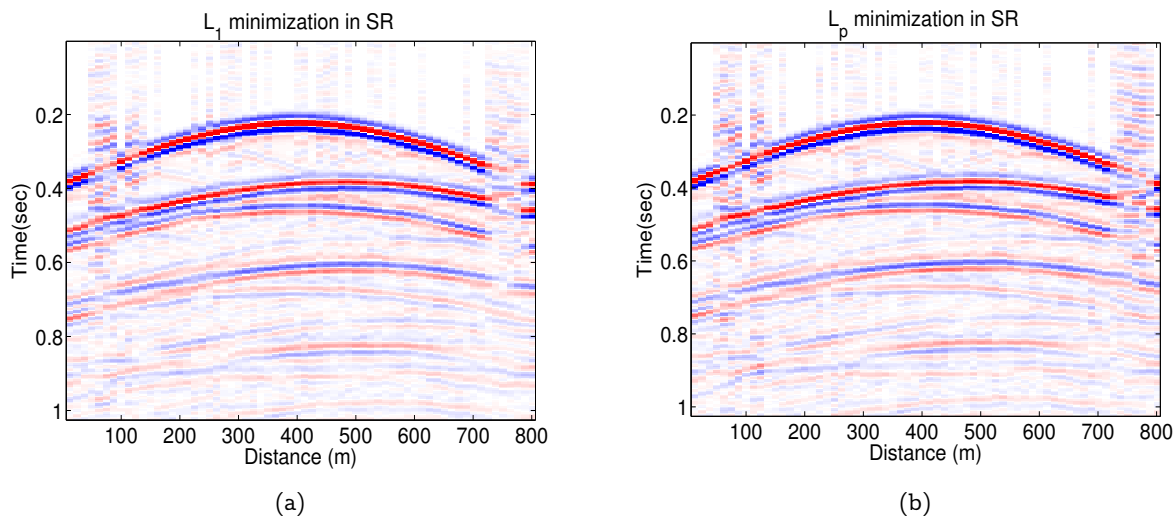


Figure 9: (a) Recovered shot gather number 32 using ℓ_1 minimization in the SR domain. (b) Recovered shot gather using ℓ_p minimization in the SR domain.

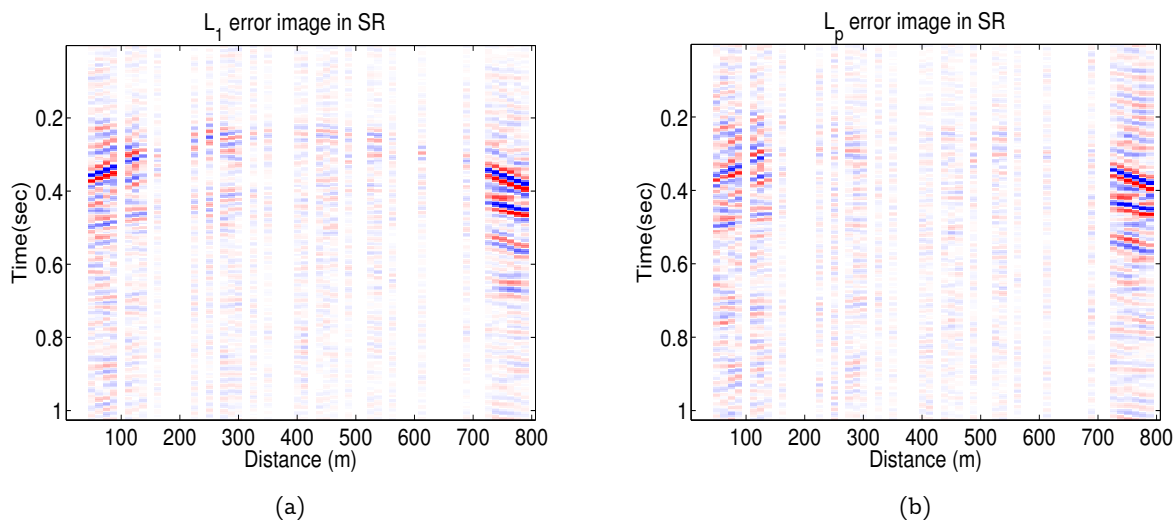


Figure 10: (a) Error plots showing the difference between the original shot gather and the reconstruction from ℓ_1 minimization in the source-receiver domain. (b) Error plots showing the difference between the original shot gather and the reconstruction from ℓ_p minimization in the SR domain.

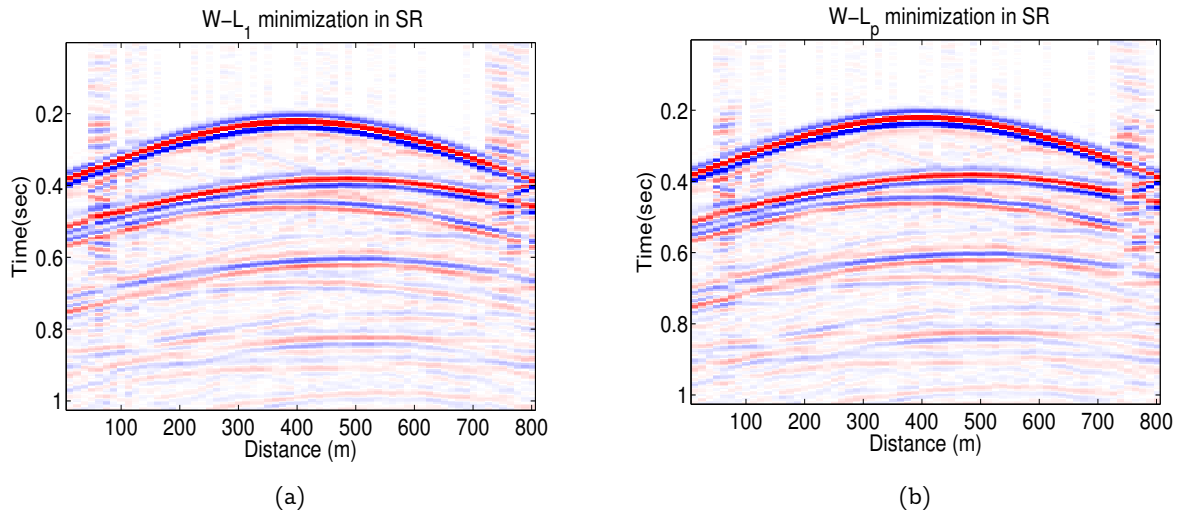


Figure 11: (a) Recovered shot gather number 32 using weighted ℓ_1 minimization in the SR domain. (b) Recovered shot gather using weighted ℓ_p minimization in the SR domain.

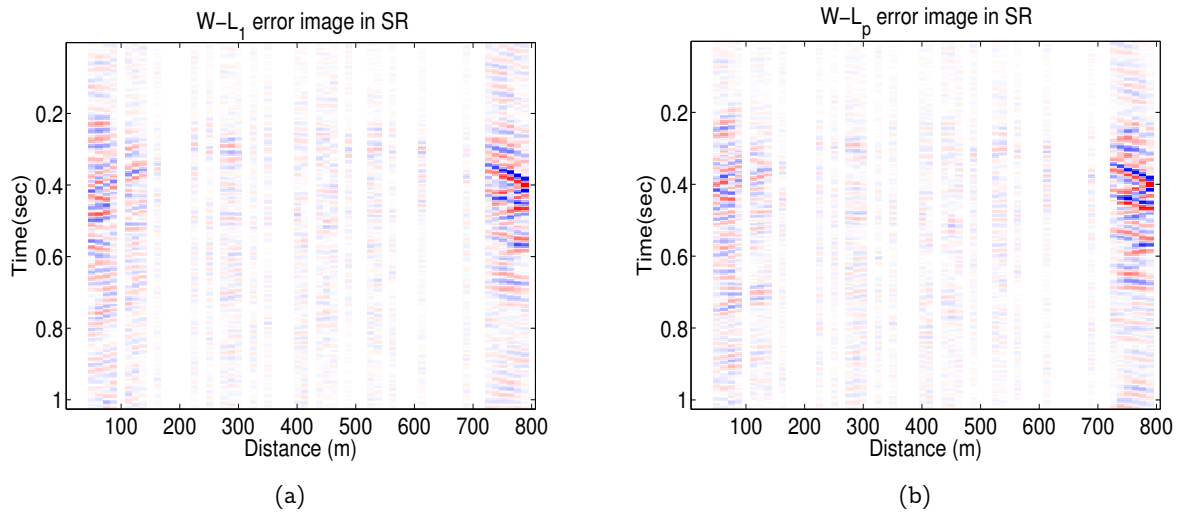


Figure 12: (a) Error plots showing the difference between the original shot gather and the reconstruction from weighted ℓ_1 minimization in the source-receiver domain. (b) Error plots showing the difference between the original shot gather and the reconstruction from weighted ℓ_p minimization in the SR domain.

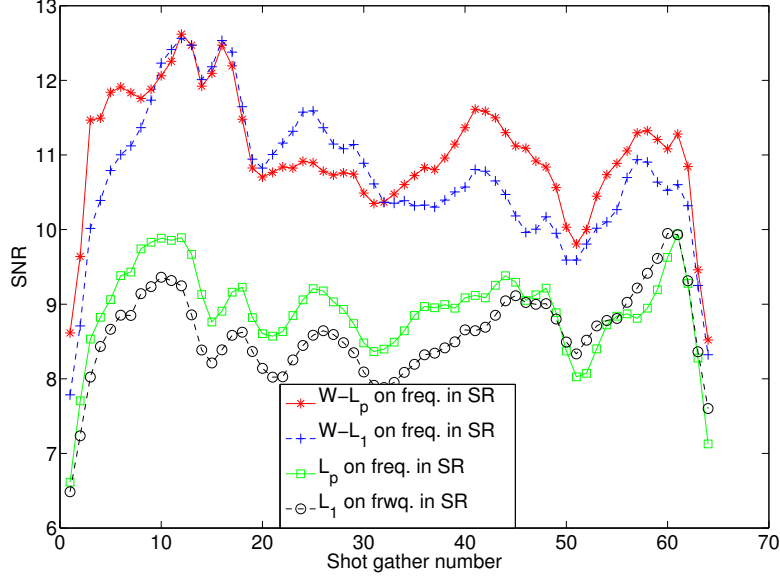


Figure 13: Comparison of the SNRs achieved by ℓ_1 , ℓ_p , weighted ℓ_1 , and weighted ℓ_p minimization in recovering shot gathers applied to source-receiver domain

6 Proof of Theorem 7

Recall that \tilde{T} , an arbitrary subset of $\{1, 2, \dots, N\}$, is of size ρk where $0 \leq \rho \leq a$ and a is some number larger than 1. Let the set $\tilde{T}_\alpha = T_0 \cap \tilde{T}$ and $\tilde{T}_\beta = T_0^c \cap \tilde{T}$ where, $|\tilde{T}_\alpha| = \alpha |\tilde{T}| = \alpha \rho k$ and $\alpha + \beta = 1$.

Let $x^* = x + h$ be a minimizer of the weighted ℓ_p problem. Then

$$\|x + h\|_{p,w} \leq \|x\|_{p,w} \Rightarrow \|x + h\|_{p,w}^p \leq \|x\|_{p,w}^p.$$

Using the weights, we have

$$\omega^p \|x_{\tilde{T}} + h_{\tilde{T}}\|_p^p + \|x_{\tilde{T}^c} + h_{\tilde{T}^c}\|_p^p \leq \omega^p \|x_{\tilde{T}}\|_p^p + \|x_{\tilde{T}^c}\|_p^p.$$

Consequently,

$$\begin{aligned} & \omega^p \|x_{\tilde{T} \cap T_0} + h_{\tilde{T} \cap T_0}\|_p^p + \omega^p \|x_{\tilde{T} \cap T_0^c} + h_{\tilde{T} \cap T_0^c}\|_p^p + \|x_{\tilde{T}^c \cap T_0} + h_{\tilde{T}^c \cap T_0}\|_p^p + \|x_{\tilde{T}^c \cap T_0^c} + h_{\tilde{T}^c \cap T_0^c}\|_p^p \\ & \leq \omega^p \|x_{\tilde{T} \cap T_0}\|_p^p + \omega^p \|x_{\tilde{T} \cap T_0^c}\|_p^p + \|x_{\tilde{T}^c \cap T_0}\|_p^p + \|x_{\tilde{T}^c \cap T_0^c}\|_p^p. \end{aligned}$$

We use the forward and reverse triangle inequalities to get

$$\omega^p \|h_{\tilde{T} \cap T_0^c}\|_p^p + \|h_{\tilde{T}^c \cap T_0^c}\|_p^p \leq \omega^p \|h_{\tilde{T} \cap T_0}\|_p^p + \|h_{\tilde{T}^c \cap T_0}\|_p^p + 2(\omega^p \|x_{\tilde{T} \cap T_0^c}\|_p^p + \|x_{\tilde{T}^c \cap T_0^c}\|_p^p).$$

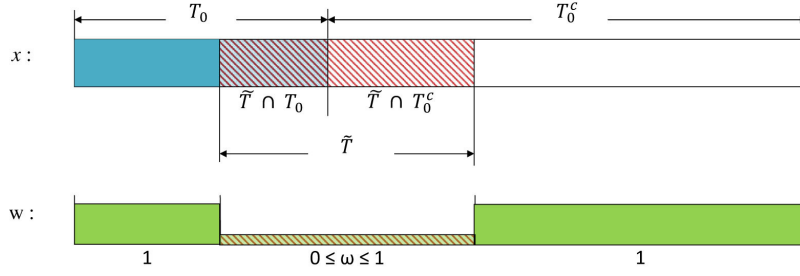


Figure 14: Illustration of the signal x and weight vector w emphasizing the relationship between the sets T_0 and \tilde{T} .

Adding and subtracting $\omega^p \|h_{\tilde{T}^c \cap T_0^c}\|_p^p$ to the left hand side and adding and subtracting $\omega^p \|h_{\tilde{T}^c \cap T_0}\|_p^p + \omega^p \|x_{\tilde{T}^c \cap T_0^c}\|_p^p$ to the right hand side we get

$$\begin{aligned} & \omega^p \|h_{\tilde{T} \cap T_0^c}\|_p^p + \omega^p \|h_{\tilde{T}^c \cap T_0^c}\|_p^p + \|h_{\tilde{T}^c \cap T_0}\|_p^p - \omega^p \|h_{\tilde{T}^c \cap T_0}\|_p^p \leq \omega^p \|h_{\tilde{T} \cap T_0}\|_p^p + \omega^p \|h_{\tilde{T}^c \cap T_0}\|_p^p \\ & + \|h_{\tilde{T}^c \cap T_0}\|_p^p - \omega^p \|h_{\tilde{T}^c \cap T_0}\|_p^p + 2(\omega^p \|x_{\tilde{T} \cap T_0^c}\|_p^p + \omega^p \|x_{\tilde{T}^c \cap T_0^c}\|_p^p + \|x_{\tilde{T}^c \cap T_0}\|_p^p - \omega^p \|x_{\tilde{T}^c \cap T_0}\|_p^p). \end{aligned}$$

Since $\|h_{T_0^c}\|_p^p = \|h_{\tilde{T} \cap T_0^c}\|_p^p + \|h_{\tilde{T}^c \cap T_0^c}\|_p^p$ we get

$$\begin{aligned} & \omega^p \|h_{T_0^c}\|_p^p + (1 - \omega^p) \|h_{\tilde{T}^c \cap T_0^c}\|_p^p \leq \omega^p \|h_{T_0}\|_p^p \\ & + (1 - \omega^p) \|h_{\tilde{T}^c \cap T_0}\|_p^p + 2(\omega^p \|x_{T_0^c}\|_p^p + (1 - \omega^p) \|x_{\tilde{T}^c \cap T_0^c}\|_p^p). \end{aligned} \quad (12)$$

We also have $\|h_{T_0^c}\|_p^p = \omega^p \|h_{T_0^c}\|_p^p + (1 - \omega^p) \|h_{\tilde{T} \cap T_0^c}\|_p^p + (1 - \omega^p) \|h_{\tilde{T}^c \cap T_0^c}\|_p^p$. Combining this with (12) we get

$$\begin{aligned} & \|h_{T_0^c}\|_p^p \leq \omega^p \|h_{T_0}\|_p^p + (1 - \omega^p) (\|h_{\tilde{T}^c \cap T_0}\|_p^p + \|h_{\tilde{T} \cap T_0^c}\|_p^p) \\ & + 2(\omega^p \|x_{T_0^c}\|_p^p + (1 - \omega^p) (\|x_{\tilde{T}^c \cap T_0^c}\|_p^p)). \end{aligned} \quad (13)$$

Define $\tilde{T}_\alpha := T_0 \cap \tilde{T}$. Then $\|h_{\tilde{T}^c \cap T_0}\|_p^p + \|h_{\tilde{T} \cap T_0^c}\|_p^p = \|h_{T_0 \cup \tilde{T} \setminus \tilde{T}_\alpha}\|_p^p$ and from (13)

$$\|h_{T_0^c}\|_p^p \leq \omega^p \|h_{T_0}\|_p^p + (1 - \omega^p) \|h_{T_0 \cup \tilde{T} \setminus \tilde{T}_\alpha}\|_p^p + 2(\omega^p \|x_{T_0^c}\|_p^p + (1 - \omega^p) (\|x_{\tilde{T}^c \cap T_0^c}\|_p^p)). \quad (14)$$

Now partition T_0^c into sets of $T_1, T_2, \dots, |T_j| = ak$ for $j \geq 1$, such that T_1 is the set of indices of the ak largest (in magnitude) coefficients of $h_{T_0^c}$ and so on. Finally let $T_{01} := T_0 \cup T_1$. Now we can find a lower bound for $\|Ah\|_2^p$ using the RIP condition of the matrix A . We have

$$\begin{aligned} \|Ah\|_2^p &= \|Ah_{T_{01}}\|_2^p + \sum_{j \geq 2} \|Ah_{T_j}\|_2^p \geq \|Ah_{T_{01}}\|_2^p - \sum_{j \geq 2} \|Ah_{T_j}\|_2^p \\ &\geq (1 - \delta_{ak+|T_0|})^{\frac{p}{2}} \|h_{T_{01}}\|_2^p - (1 + \delta_{ak})^{\frac{p}{2}} \sum_{j \geq 2} \|h_{T_j}\|_2^p. \end{aligned} \quad (15)$$

Here we also use the fact that $\|\cdot\|_2^p$ satisfies the triangle inequality for $0 < p < 1$. Now we should note that $|h_{T_{j+1}}(l)|^p \leq |h_{T_j}(l')|^p$ for all $l \in T_{j+1}$ and $l' \in T_j$, and thus $|h_{T_{j+1}}(l)|^p \leq \frac{\|h_{T_j}\|_p^p}{ak}$. It follows that $\|h_{T_j}\|_2^2 \leq (ak)^{1-\frac{2}{p}}\|h_{T_j}\|_p^2$ and consequently

$$\sum_{j \geq 2} \|h_{T_j}\|_2^p \leq (ak)^{\frac{p}{2}-1} \sum_{j \geq 1} \|h_{T_j}\|_p^p = (ak)^{\frac{p}{2}-1} \|h_{T_0^c}\|_p^p. \quad (16)$$

Using (16) in (15) we get

$$\|Ah\|_2^p \geq (1 - \delta_{ak+|T_0|})^{\frac{p}{2}} \|h_{T_0}\|_2^p - (1 + \delta_{ak})^{\frac{p}{2}} (ak)^{\frac{p}{2}-1} \|h_{T_0^c}\|_p^p. \quad (17)$$

Next, consider the feasibility of x^* and x . Both vectors are feasible, so we have $\|Ah\|_2 \leq 2\varepsilon$. Also note that $|T_0 \cup \tilde{T} \setminus \tilde{T}_\alpha| = (1 + \rho - 2\alpha\rho)k$ and $\|h_{T_0}\|_p^p \leq |T_0|^{1-\frac{p}{2}} \|h_{T_0}\|_2^p$. Using these and (14) in (17) we get

$$\begin{aligned} (1 - \delta_{ak+|T_0|})^{\frac{p}{2}} \|h_{T_0}\|_2^p &\leq (2\varepsilon)^p + 2(1 + \delta_{ak})^{\frac{p}{2}} (ak)^{\frac{p}{2}-1} (\omega^p \|x_{T_0^c}\|_p^p + (1 - \omega^p) \|x_{\tilde{T}^c \cap T_0^c}\|_p^p) + \\ &(1 + \delta_{ak})^{\frac{p}{2}} (ak)^{\frac{p}{2}-1} (\omega^p |T_0|^{1-\frac{p}{2}} \|h_{T_0}\|_2^p + (1 - \omega^p) ((1 + \rho - 2\alpha\rho)k)^{1-\frac{p}{2}} \|h_{T_0 \cup \tilde{T} \setminus \tilde{T}_\alpha}\|_2^p). \end{aligned} \quad (18)$$

T_1 contains the largest ak coefficients of $h_{T_0^c}$ with $a > 1$. So $|\tilde{T} \setminus \tilde{T}_\alpha| = (1 - \alpha)\rho k \leq ak$ then $\|h_{T_0 \cup \tilde{T} \setminus \tilde{T}_\alpha}\|_2 \leq \|h_{T_0}\|_2$.

Defining $E_\omega := (\omega^p \|x_{T_0^c}\|_p^p + (1 - \omega^p) \|x_{\tilde{T}^c \cap T_0^c}\|_p^p)$ and $S_\omega := (\omega^p |T_0|^{1-\frac{p}{2}} + (1 - \omega^p) ((1 + \rho - 2\alpha\rho)k)^{1-\frac{p}{2}})$ and using $\|h_{T_0}\|_2 \leq \|h_{T_0}\|_2$ we have

$$\|h_{T_0}\|_2^p \leq \frac{(2\varepsilon)^p + 2(1 + \delta_{ak})^{\frac{p}{2}} (ak)^{\frac{p}{2}-1} E_\omega}{(1 - \delta_{ak+|T_0|})^{\frac{p}{2}} - (1 + \delta_{ak})^{\frac{p}{2}} (ak)^{\frac{p}{2}-1} S_\omega}. \quad (19)$$

To complete the proof denote by $h_{T_0^c}[m]$ the m -th largest coefficient of $h_{T_0^c}$ and observe that $|h_{T_0^c}[m]|^p \leq \frac{\|h_{T_0^c}\|_p^p}{m}$. As $h_{T_0^c}[m] = h_{T_0^c}[m + ak]$ we have:

$$\|h_{T_0^c}\|_2^2 = \sum_{m \geq ak+1} |h_{T_0^c}[m]|^2 \leq \sum_{m \geq ak+1} \left(\frac{\|h_{T_0^c}\|_p^p}{m}\right)^{\frac{2}{p}} \leq \frac{\|h_{T_0^c}\|_p^2}{(ak)^{\frac{2}{p}-1} \left(\frac{2}{p} - 1\right)}. \quad (20)$$

The last inequality follows because for $0 < p < 1$:

$$\sum_{m \geq ak+1} m^{-\frac{2}{p}} \leq \int_{ak}^{\infty} t^{-\frac{2}{p}} dt = \frac{1}{(ak)^{\frac{2}{p}-1} \left(\frac{2}{p} - 1\right)}.$$

Combining (20) with (14) we get

$$\begin{aligned} \|h_{T_0^c}\|_2^p &\leq \left((ak)^{\frac{2}{p}-1} \left(\frac{2}{p} - 1\right)\right)^{-\frac{p}{2}} (\omega^p \|h_{T_0}\|_p^p + \\ &(1 - \omega^p) \|h_{T_0 \cup \tilde{T} \setminus \tilde{T}_\alpha}\|_p^p + 2(\omega^p \|x_{T_0^c}\|_p^p + (1 - \omega^p) (\|x_{\tilde{T}^c \cap T_0^c}\|_p^p))). \end{aligned} \quad (21)$$

We showed that $\|h_{T_0 \cup \tilde{T} \setminus \tilde{T}_\alpha}\|_2 \leq \|h_{T_{01}}\|_2$ and $\|h_{T_0}\|_2 \leq \|h_{T_{01}}\|_2$.

Using these in (21) we get

$$\begin{aligned} \|h_{T_{01}^c}\|_2^p &\leq ((ak)^{\frac{2}{p}-1} (\frac{2}{p} - 1))^{-\frac{p}{2}} * \left((\omega^p |T_0|^{1-\frac{p}{2}} + (1 - \omega^p)((1 + \rho - 2\alpha\rho)k)^{1-\frac{p}{2}}) \|h_{T_{01}}\|_2^p \right. \\ &\quad \left. + 2 \left(\omega^p \|x_{T_0^c}\|_p^p + (1 - \omega^p) (\|x_{\tilde{T}^c \cap T_0^c}\|_p^p) \right) \right). \end{aligned} \quad (22)$$

We can find a bound for $\|h\|_2$ using (19) and (22)

$$\begin{aligned} \|h\|_2^2 &= (\|h_{T_{01}}\|_2^p)^{\frac{2}{p}} + (\|h_{T_{01}^c}\|_2^p)^{\frac{2}{p}} \leq \left(\|h_{T_{01}}\|_2^p + \|h_{T_{01}^c}\|_2^p \right)^{\frac{2}{p}}. \quad (23) \\ \|h\|_2^p &\leq \frac{2^p \left(1 + \frac{S_\omega}{\left((ak)^{\frac{2}{p}-1} (\frac{2}{p}-1) \right)^{\frac{p}{2}}} \right) \varepsilon^p}{(1 - \delta_{ak+|T_0|})^{\frac{p}{2}} - (1 + \delta_{ak})^{\frac{p}{2}} (ak)^{\frac{p}{2}-1} E_\omega} + \frac{2 \left((1 + \delta_a)^{\frac{p}{2}} a^{\frac{p}{2}-1} + \frac{(1 - \delta_{(a+1)k})^{\frac{p}{2}}}{\left(a^{\frac{2}{p}-1} (\frac{2}{p}-1) \right)^{\frac{p}{2}}} \right) E_\omega}{(1 - \delta_{ak+|T_0|})^{\frac{p}{2}} - (1 + \delta_{ak})^{\frac{p}{2}} (ak)^{\frac{p}{2}-1} S_\omega}, \quad (24) \end{aligned}$$

with the condition that the denominator is positive, equivalently:

$$\delta_{ak} + \frac{a^{\frac{2}{p}-1}}{(\omega^p + (1 - \omega^p)(1 + \rho - 2\alpha\rho)^{1-\frac{p}{2}})^{\frac{2}{p}}} \delta_{(a+1)k} < \frac{a^{\frac{2}{p}-1}}{(\omega^p + (1 - \omega^p)(1 + \rho - 2\alpha\rho)^{1-\frac{p}{2}})^{\frac{2}{p}}} - 1. \quad (25)$$

ACKNOWLEDGEMENT

This work was supported in part by the Natural Sciences and Engineering Research Council of Canada (NSERC) Discovery Grant (22R82411), the NSERC Accelerator Award (22R68054) and the NSERC Collaborative Research and Development Grant DNOISE II (22R07504). This research was carried out as part of the SINBAD II project with support from the following organizations: BG Group, BP, BGP, Chevron, ConocoPhillips, Petrobras, PGS, Total SA, WesternGeco, Woodside, Ion, and CGG.

References

- [1] Bubacarr Bah and Jared Tanner. Improved bounds on restricted isometry constants for gaussian matrices. *CoRR*, 2010.
- [2] E. J. Candès, J. Romberg, and T. Tao. Stable signal recovery from incomplete and inaccurate measurements. *Communications on Pure and Applied Mathematics*, 59:1207–1223, 2006.
- [3] R. Chartrand and Wotao Tin. Iteratively reweighted algorithms for compressive sensing. *IEEE International Conference on Acoustics, Speech and Signal Processing (ICASSP), 2008.*, pages 3869–3872, 31 2008-April 4 2008.

- [4] Rick Chartrand. Exact reconstructions of sparse signals via nonconvex minimization. *IEEE Signal Processing Letters*, 14(10):707–710, 2007.
- [5] Xiaojun Chen and Weijun Zhou. Convergence of reweighted ℓ_1 minimization algorithms and unique solution of truncated ℓ_p minimization.
- [6] L. Demanet and E. J. Candés. The curvelet representation of wave propagators is optimally sparse. volume 58, pages 1472–1528, 2005.
- [7] D. Donoho. Compressed sensing. *IEEE Transactions on Information Theory*, 52(4):1289–1306, 2006.
- [8] D. Donoho and M. Elad. Optimally sparse representation in general (nonorthogonal) dictionaries via ℓ^1 minimization. *Proceedings of the National Academy of Sciences of the United States of America*, 100(5):2197–2202, 2003.
- [9] Q. Du and J. E. Fowler. Hyperspectral image compression using jpeg2000 and principal component analysis. *IEEE Geosci. Remote Sens. Lett.*, 4, no. 4:201–205, April 2007.
- [10] S. Foucart and M.J. Lai. Sparsest solutions of underdetermined linear systems via ℓ^q -minimization for $0 < q \leq 1$. *Applied and Computational Harmonic Analysis*, 26(3):395–407, 2009.
- [11] Michael P. Friedlander, Hassan Mansour, Rayan Saab, and Özgür Yılmaz. Recovering compressively sampled signals using partial support information. *IEEE Transactions on Information Theory*, 58(2):1122–1134, 2012.
- [12] G. Hennenfent and F. Herrmann. Simply denoise: wavefield reconstruction via jittered undersampling. *Geophysics*, 73:V19, 2008.
- [13] F. J. Herrmann, P. P. Moghaddam, and C. C. Stolk. Sparsity- and continuity- promoting seismic imaging with curvelet frames. *Journal of Applied and Computational Harmonic Analysis*, 24:150–173, 2008.
- [14] M. Lustig, D. Donoho, and J.M. Pauly. Sparse MRI: The Application of Compressed Sensing for Rapid MR Imaging. *Preprint*, 2007.
- [15] Hassan Mansour, Felix J Herrmann, and O Yilmaz. Improved wavefield reconstruction from randomized sampling via weighted one-norm minimization. *submitted to Geophysics, GEO-2012-0383*, 78, no. 5:V193–V206, 2012.
- [16] R. Saab, R. Chartrand, and O. Yilmaz. Stable sparse approximations via nonconvex optimization. In *IEEE International Conference on Acoustics, Speech and Signal Processing (ICASSP)*, pages 3885–3888, 2008.

- [17] Rayan Saab and Özgür Yılmaz. Sparse recovery by non-convex optimization -instance optimality. *Applied and Computational Harmonic Analysis*, 29(1):30–48, 2010.